International Journal of Electrical, Electronic and Communication Sciences
ISSN: 2517-9438
Vol:11, No:9, 2017

# BLDC Motor Driven for Solar Photo Voltaic Powered Air Cooling System

D. Shobha Rani, M. Muralidhar

***Abstract*—**Solar photovoltaic (SPV) power systems can be employed as electrical power sources to meet the daily residential energy needs of rural areas that have no access to grid systems. In view of this, a standalone SPV powered air cooling system is proposed in this paper, which constitutes a dc-dc boost converter, two voltage source inverters (VSI) connected to two brushless dc (BLDC) motors which are coupled to a centrifugal water pump and a fan blower. A simple and efficient Maximum Power Point Tracking (MPPT) technique based on Silver Mean Method (SMM) is utilized in this paper. The air cooling system is developed and simulated using the MATLAB / Simulink environment considering the dynamic and steady state variation in the solar irradiance.

***Keywords*—**Boost converter, solar photovoltaic array, voltage source inverter, brushless DC motor, solar irradiance, Maximum Power Point Tracking, Silver Mean Method.

## I. Introduction

GLOBALLY, the rate of energy consumption has increased significantly, due to increase in population, industrialization and transportation and the supply is not matching with the growing demand for energy . The growing energy demands and limited domestic fossil fuel reserves led to the depletion of these conventional energy sources. The limited availability of these energy sources, paved to explore the use of renewable sources. More ways are being explored to tap renewable sources in the optimum way possible which makes these sources a more lucrative option from futuristic perspective [1]–[3]. Among all the renewable energy resources available, solar energy is the most abundant and the effective harvest of this can easily fulfill present energy demand of world. Its limitless availability and easy accessibility makes it a more viable option. With the falling prices of solar PV panels, generating solar energy has become feasible [4], [5].

In recent years, BLDC motors have gained popularity in a plethora of applications. The BLDC motor is far more dependable than the DC motor because it uses an electronic commutator instead of a mechanical commutator. The advantages of brushless motors over brushed DC motors include: better speed versus torque characteristics, high efficiency and reliability, noiseless operation, longer lifetime, eradication of ionizing sparks from the commutator and an altogether trimming of electromagnetic interference (EMI). Due to all above paramount advantages, BLDC motor has been chosen to develop SPV fed air cooler [6], [7].

Maximum efficiency of the SPV array is attained via a maximum power point tracking (MPPT) algorithm using the DC-DC converters. Numerous DC-DC converters have been employed for MPPT in different SPV array based applications. However, most of the classical converter topologies have the highest values of reactive components resulting in an increased cost, size and weight and therefore, in the proposed system, a boost converter with desired features such as good switch utilization, high conversion efficiency, low stress on semiconductor devices and minimal number of reactive elements is selected [6], [7]. The SPV array is chosen such that its MPP always occurs within the bounded MPP region of the boost converter so that the power is invariably optimized immaterial of the variation in solar irradiance and loading conditions.MPPT techniques are employed to track maximum power from the SPV system and to increase the energy efficiency. The major drawbacks associated with the traditional MPPT techniques are low conversion efficiency and slow response. To overcome these problems, a simple and efficient MPPT algorithm based on SMM is presented in this paper. The proposed algorithm operates in a given interval and converges to MPP of the SPV system by shrinking its interval. After achieving the maximum power, the algorithm stops shrinking and maintains constant voltage until the next interval is decided [8], [9].

The structure of the paper is as follows: First section provides the introduction of the paper. Section II describes the various stages in the configuration of the proposed system and Section III deals with the design of the PV array. Sections IV and V discuss about the design of DC-DC boost converter. Section VI illustrates the BLDC motor drive system and Section VII presents the control techniques of the system. Section VIII shows the results and the simulation work carried through MATLAB/Simulink and the final section exemplifies the conclusion.

## II. Proposed System Description

The description of the SPV based boost converter fed BLDC motor drive for air cooling system is depicted in Fig. 1. The solar panel output is given to the DC-DC boost converter through the SMM based MPPT controller and output of the boost converter is given to two VSI's which are fed to two BLDC motors to drive the centrifugal water pump and a fan blower. The detailed designs of various stages such as SPV array DC-DC boost converter, SPWM technique based

D. Shobha Rani is with the Department of Electrical and Electronics Engineering, Institute of Aeronautical Engineering, Hyderabad, India (e-mail: depuru_shobha@yahoo.com).
Muralidhar M. is with the Department of Electrical and Electronics Engineering, S. V. University College of Engineering, Tirupati, India (e-mail: muralidhar6666@gmail.com).

inverter, BLDC motor driven centrifugal water pump and fan blower are described as follows.

## III. Design of PV Array

The conversion of solar energy to electrical energy is done through solar PV cells. To increase the output voltage or the output current, the PV cells are connected in series or parallel combinations to form solar arrays. The equivalent circuit of a practical PV cell is shown in Fig. 2, which consists of a current source $I_{ph}$, a series resistance Rs and a parallel resistance $R_{sh}$ [2].

The capacity of SPV array is selected slightly greater than that of the BLDC-motors, which perpetuates the smooth functioning of the proposed system despite the power losses. Hence, the selected capacity of SPV array is $P_{mpp} = 1000\ W$ which is slightly more than what is required by the motors and also, all its parameters are framed accordingly. The voltage of the SPV array at MPP is selected considering BLDC motor voltage rating which is similar to the VSI DC link voltage rating. Table I summarizes the estimation of the various parameters to design an SPV array of appropriate size [10].

TABLE I
Design of SPV Array

| | |
|---|---|
| **SPV Module** | |
| Peak power, $P_m\ (W)$ | 330 |
| Open circuit voltage, $V_o\ (V)$ | 44.5 |
| Short circuit current, $I_s\ (A)$ | 8.83 |
| Operating Temperature ($^\circ c$) | 25 |
| Number of modules in a cell, $N_{ss}$ | 72 |
| Series resisitance ($\Omega$) | 0.101 |
| Parallel resistance ($\Omega$) | 1200 |
| **SPV Array** | |
| Power at MPP, $P_{mpp}$ (W) | 1000 |
| Voltage at MPP, $V_m\ (V)$ | 113 |
| Current at MPP, $I_m\ (A)$ | 8.85 |
| Number of strings in series | 3 |
| Number of strings in parallel | 1 |

## IV. Design of Boost Converter

SPV systems require the use of DCDC converters to regulate and control the sporadic output of the solar panel. In addition, the boost converter topology is the only one that allows follow up of the PV array MPP notwithstanding the temperature, irradiance, and connected load [7]. The SPV array voltage at MPP, $V_{pv} = 113\ V$ appears as the input voltage source, whereas DC link voltage of VSI, $V_{dc} = 150\ V$ appears as the output voltage of the boost converter. The duty ratio, D, of the boost converter is evaluated by employing the input-output relationship [11] as shown in (1).

$$D = \frac{V_{dc}}{V_{dc} + V_{pv}} = 0.57 \tag{1}$$

The average current flowing through the DC link, $I_{dc}$ is estimated by (2)

$$I_{dc} = \frac{P_{mpp}}{V_{dc}} = 6.67\ A \tag{2}$$

The design calculations of inductor L and DC link capacitor C [6] are done as shown in Table II.

TABLE II
Design of Boost Converter

| Parameter | Equation | Design values | Parameter Value | Selected parameter value |
|---|---|---|---|---|
| L | $\frac{D*V_{pv}}{f*\Delta I_L}$<br>$I_L = N_p * I_m$ | $D = 0.57$<br>$V_{pv} = 113\ V$<br>$f_{sw} = 20\ KHz$<br>$N_p = 1$<br>$I_m = 8.83\ A$<br>$\Delta I_L = 1\%\ of\ I_L$ | $5.432\ mH$ | $5.4\ mH$ |
| C | $\omega = 2 * \pi * f$<br>$= \frac{2*\pi N_r * P}{120}$<br>$C = \frac{I_{dc}}{6*\omega*\Delta V_{dc}}$ | $P = 4$<br>$N_{rated} = 1000\ rpm$<br>$I_{dc} = 6.67\ A$<br>$V_{dc} = 150\ V$<br>$\Delta V_{dc} = 1\%\ of\ V_{dc}$ | $1500\ \mu F$ | $1500\ \mu F$ |

## V. Design of BLDC Motor Drive

### A. Design of BLDC Motor

BLDC motors are considered to have various advantages [12]–[14] and hence are used to develop a SPV fed air cooler, which can operate satisfactorily for longer time.

Since the conventional drive circuits are expensive, bulky and complex, this paper proposes a low cost, compact, user friendly and high performance BLDC drive system which employs solar module. The practical converters undergo various power losses and the functioning of the BLDC motors is affected by the mechanical and electrical losses associated with them. To compensate these losses, the maximum power capacity of SPV array is selected slightly more than that of the BLDC motors which facilitates the flawless operation of the proposed system despite the power losses [13], [14]. The parameters and ratings of the BLDC motor selected for the proposed system are indicated in the Table III.

TABLE III
Specifications of BLDC Motor

| | |
|---|---|
| Power $P\ (W)$ | 500 |
| Speed, $N_r\ (rpm)$ | 1000 |
| DC voltage, $V_{dc}\ (V)$ | 200 |
| No. of poles $P$ | 4 |
| Moment of inertia, $J\ (Kg\dot{c}m^2)$ | 0.19 |
| Current, $I_s\ (A)$ | 2.5 |
| Voltage constant, $K_e\ (V/K_{rpm})$ | 75 |
| Torque constant, $K_t\ (N_m/A)$ | 2.16 |
| phase/phase resistance, $R_s\ (\Omega)$ | 0.2 |
| phase/phase inductance, $L_s\ (mH)$ | 8.5 |

### B. Design of Water Pump

One of the BLDC motors is coupled to the water pump which is driven as a load to the BLDC motor by giving a load-torque signal depending on the torque-speed characteristic equation of a pump [15]. The rating of the pump is taken as $0.4\ KW$ and the estimation of proportionality constant, $K_p$ for the selected water pump is taken by its torque-speed characteristics (3)

$$T_p = K_p \omega_p^2 \tag{3}$$

Where p is the mechanical speed of the rotor in $rad/sec$ and $T_p$ is the electromagnetic torque developed by the BLDC motor under steady state for stable operation. With the given power rating, the proportionality constant, $K_p$ for the

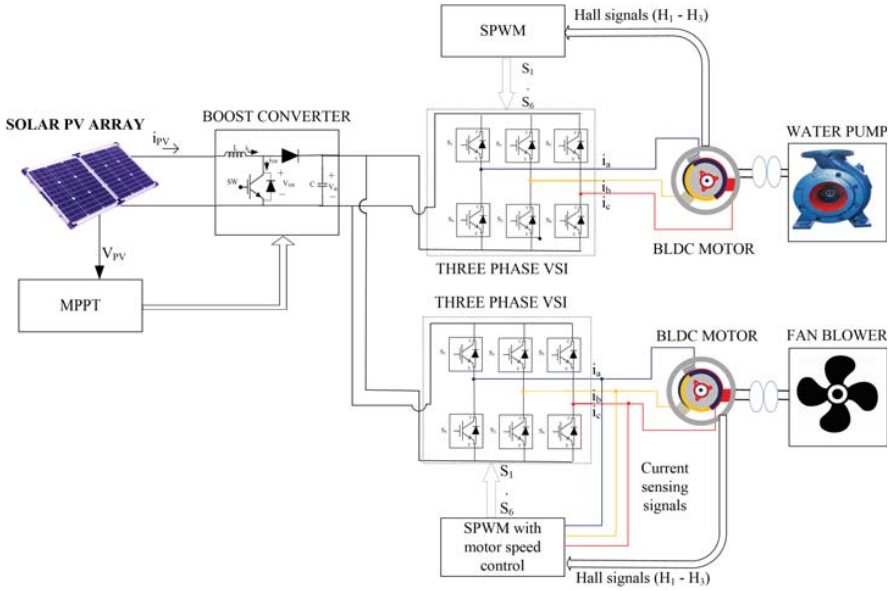


Fig. 1 Proposed SPV fed air cooling system

selected water pump is given by the equation. The detailed specifications of the centrifugal water pump are given in Table IV.

TABLE IV
SIMULINK PARAMETERS OF CENTRIFUGAL WATER PUMP

| | |
|---|---|
| Number of Phases | 3 |
| Back EMF waveform | Trapezoidal |
| Mechanical Input | Torque $T_m$ |
| Stator Phase resistance $R_s$ $(\Omega)$ | 2.8750 |
| Stator phase inductance $L_s$ $(H)$ | $8.5e^{-03}$ |
| Flux linkage established by magnets $(V \cdot s)$ | 0.175 |
| Voltage Constant $(V_{peak}/K_{rpm})$ | 146.6077 |
| Torque constant $(N \cdot m/A_{peak})$ | 1.4 |
| Back EMF flat area $(degrees)$ | 120 |
| Inertia $(J \cdot Kg \cdot m^2)$ | $0.8e^{-03}$ |
| Viscous damping | $1e^{-03}$ |
| Pole pairs | 1 |

### C. Design of Fan Blower

A fan blower is realised as a load to the second BLDC-motor and its torque-speed characteristics is related with (4),

$$T_b = K_b \omega_b^2 \tag{4}$$

Where, Tb is the load torque offered by the blower which is equal to the electromagnetic torque developed by the BLDC motor under steady state for stable operation and b is the mechanical speed of the rotor in $rad/sec$. To estimate the proportionality constant, $K_b$ for the selected blower, the equation given below is utilized.

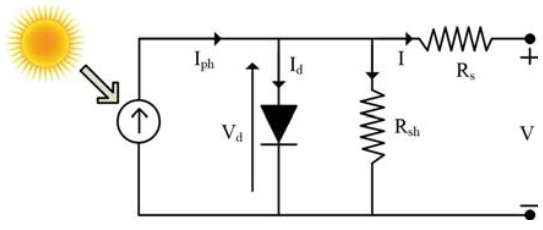


Fig. 2 PV Cell Equivalent Circuit

## VI. CONTROL SCHEMES OF THE PROPOSED SYSTEM

The air cooling system proposed is controlled through three control schemes viz. SMM based MPPT Controller, electronic commutation and DC-link voltage controller [12]. These schemes are detailed as follows:

### A. SMM Based MPPT Algorithm

The salient features of all solar panels include a distinct maximum power point (MPP) and a nonlinear voltage-current characteristic, which relies on the atmospheric conditions, such as temperature and irradiance. In order to continuously harvest maximum power from the solar panels, they have to be operated at their MPP despite the inevitable changes in the environment. The solar to electrical energy conversion efficiency of solar cell lies between 9-20%. Hence, it is important to use MPPT controller to enhance the overall efficiency of system [11], [16], [17]. A classical technique based on silver mean is proposed in this paper for optimizing the functions. Silver mean of two quantities is defined as the ratio of the sum of the smaller and twice the larger of those quantities, to the larger quantity, which is the same as the ratio of the larger to the smaller quantity. Let a be the larger quantity and b the smaller quantity in a search area and let $\alpha_S$

be the silver mean constant. Mathematically, it is expressed by the following equations from (5)-(8)

$$\frac{2a+b}{a} = \frac{a}{b} = \alpha_S \tag{5}$$

$$2 + \frac{b}{a} = \frac{a}{b} = \alpha_S \tag{6}$$

$$2 + \frac{1}{\alpha_S} = \alpha_S \tag{7}$$

$$\alpha_S^2 - 2\alpha_S - 1 = 0 \tag{8}$$

The silver mean $\alpha_S$ conjugate value is 0.41, which is obtained from the ratios of larger and smaller quantities. Using the conjugate value the optimization function is chosen from P-V curve as a closed interval [a, b] which is equal to [0, $V_{OC}$]. Since MPP of the PV system always stays close to the open interval, it can be further reduced from the left of the P-V curve. Initially the two voltages $V_1$ and $V_2$ obtained in the interval [a, b] are given as in (9) and (10).

$$V_1 = a + 0.41(b-a) \tag{9}$$

$$V_2 = b - 0.41(b-a) \tag{10}$$

Corresponding powers at P($V_1$) and P($V_2$) are obtained from the PV system. By comparing the obtained powers, the interval shrinks either to [a, $V_1$] or [b, $V_2$]. The iterations are further continued until the condition $V_2 - V_1 \leq \varepsilon$ is satisfied. The algorithm for the proposed SMM based MPPT is shown in Fig. 5. This algorithm operates in a given interval and converges to MPP of the PV system by shrinking its interval. After achieving MPP, the proposed algorithm stops shrinking and maintains constant voltage until the next interval is decided. The proposed MPPT controller can thus be used to track the maximum power. This algorithm has an advantage over P&O in that it can determine when the MPPT controller has reached the MPP, whereas P&O oscillates around the MPP. Also, this method can track the rapidly increasing and decreasing irradiance conditions with higher accuracy than P&O. The flow chart of the SMM method is shown in Fig. 3.

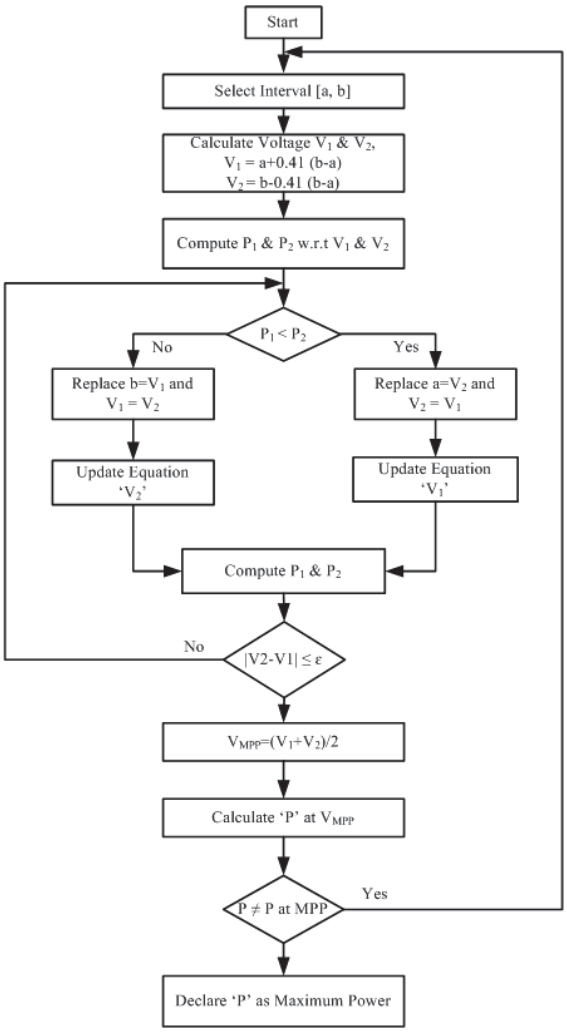


Fig. 3 Flow chart of the proposed MPPT algorithm

TABLE V
SWITCHING STATES FOR ELECTRONIC COMMUTATION OF BLDC MOTOR

| 0° | Hall Signals | | | Switching States | | | | | |
|---|---|---|---|---|---|---|---|---|---|
| | $H_1$ | $H_2$ | $H_3$ | $S_1$ | $S_2$ | $S_3$ | $S_4$ | $S_5$ | $S_6$ |
| NA | 0 | 0 | 0 | 0 | 0 | 0 | 0 | 0 | 0 |
| 0-60 | 1 | 0 | 1 | 1 | 0 | 0 | 1 | 0 | 0 |
| 60-120 | 0 | 0 | 1 | 1 | 0 | 0 | 0 | 0 | 1 |
| 120-180 | 0 | 1 | 1 | 0 | 0 | 1 | 0 | 0 | 1 |
| 180-240 | 0 | 1 | 0 | 0 | 1 | 1 | 0 | 0 | 0 |
| 240-300 | 1 | 1 | 0 | 0 | 1 | 0 | 0 | 1 | 0 |
| 300-360 | 1 | 0 | 0 | 0 | 0 | 0 | 1 | 1 | 0 |
| NA | 1 | 1 | 1 | 0 | 0 | 0 | 0 | 0 | 0 |

### B. Electronic Commutation

Electronic commutation of BLDC motors produces the switching signals for the VSI and decodes three Hall effect signals which are produced by an inbuilt encoder of the motor depending on the angular position of the rotor. BLDC motors need to operate more efficiently to reduce the energy and save cost. Moreover, to ensure greater efficiency, the correct Hall-effect sensors need to be selected for electronic commutation. These Hall effect signals are logically converted into 6 switching pulses which are further used to operate the 6 IGBT switches of the VSI. Table V depicts the switching states of VSI for each set of Hall-effect signal states.

For the fan blower, the hysteresis control method is used to obtain a preset speed . The reference speed when compared with the original speed of the BLDC motor, generates a torque reference which when divided by the constant $K_b$ obtained from (4) gives the current reference magnitude. To get current reference, this current reference magnitude is multiplied with current pattern generated through the Hall signals. The three current references such produced are then compared with the actual current flowing in the stator and the error signal is then made to pass through the proportional integral (PI) controller

which then generates two pulses each. Hence, the 6 pulses generated are given to the gates of the VSI switches resulting in a desired speed of the BLDC motor. The speed of the BLDC-motor for the water pump is regulated through the DC link voltage and the speed is fixed without using any external controlling circuit. Hence, by maintaining the power balance, it is ensured that the DC link voltage remains within limits.

### C. DC-Link Voltage Controller

If only the air blower is to be operated and no controller is used, then the DC-link voltage increases gradually due to the lack of power balance. Hence to restrict this, the power balance (Generated power = Power consumed + losses) should be maintained.

And the correct assessment of the losses is formidable. Now with the help of the DC-link voltage controller, the DC-link voltage is maintained; but this makes the SPV to be operated below MPP if the voltage reference to the DC-link voltage controller is other than Vmpp. Hence, less power is obtained. However, this will not give rise to a difficult condition as the mechanical load specified to be driven now is also diminished.

## VII. Summary of Simulation Results

Performance evaluation of the proposed air cooler is carried out using simulated results in MATLAB/Simulink considering the starting and steady state condition at the standard solar irradiance of $1000\ W/m^2$ and $600\ W/m^2$.

### A. Starting and Steady State Performances of BLDC Motor Drive System at Solar Irradiance of $1000\ W/m^2$

The various performance indices of SPV array, boost converter, BLDC motor drive connected to the two loads at a steady state solar irradiance of $1000\ W/m^2$ are illustrated in Figs. 5-10, and elaborated in the following sub-sections.

*1) Performance of SPV Array at Steady State Irradiance of $1000\ W/m^2$:* Fig. 4 shows the output parameters of the PV array viz; PVpower, PVcurrent and PVvoltage and the tracking performance of the P&O MPPT technique under the steady state condition of irradiance of $1000\ W/m^2$. These indices correspond to the operation of the SPV array at MPP as PV power reaches $1000\ W$ at steady state.

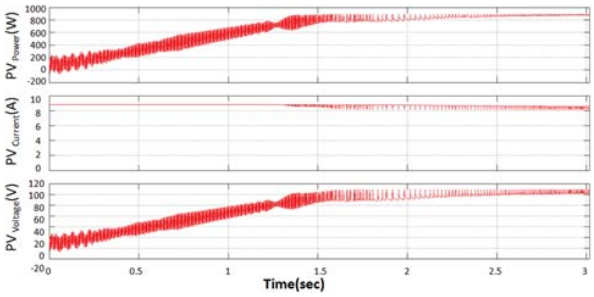


Fig. 4 Output parameters of the PV at irradiance of $1000\ W/m^2$

*2) Performance of Boost Converter at $1000\ W/m^2$:* The behaviour of the boost converter at $1000\ W/m^2$ is shown in Fig. 5. where the DC link voltage is presented. It is inferred from waveforms that the converter operates in CCM, resulting in a limited stress on the semiconductor devices.

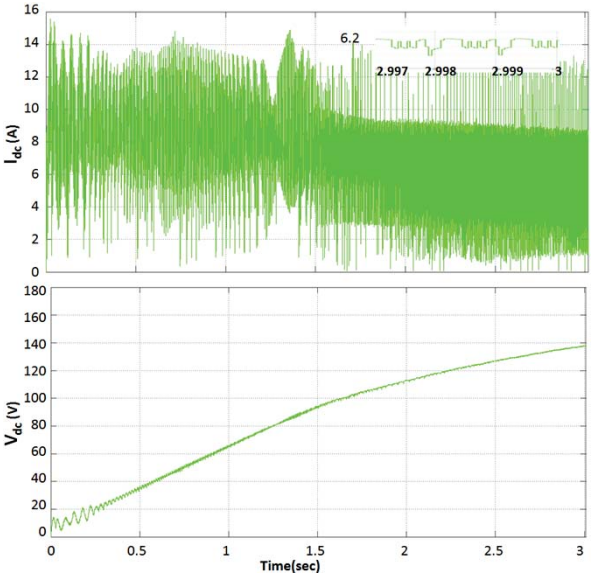


Fig. 5 Output parameters of boost converter at irradiance of $1000\ W/m^2$

*3) Performance of BLDC Motor at Steady State Irradiance of $1000\ W/m^2$:* The starting and steady state behaviours of the BLDC motor pump and motor fan at $1000\ W/m^2$ are shown in Figs. 6 and 7. All the motor indices such as the back EMF, the stator current, the speed, the electromagnetic torque and the output power offered by pump and fan reach their rated values under steady state condition as MPP is tracked. The two motors draws their rated current and attains the rated speed, resulting in the water pumping and fan operating with full capacity. The starting current of BLDC motor is bounded within the permissible range hence the motor has a soft start.

### B. Starting and Steady State Performances of BLDC Motor Drive System at Solar Irradiance of $600\ W/m^2$

The various performance indices of SPV array, boost converter and BLDC motor drive system under starting and steady state at the standard solar irradiance of $600\ W/m^2$ are illustrated in Figs. 9-12, and elaborated in the following sub-sections. All the indices reach their rated values at this solar irradiance.

*1) Performance of SPV Array at Steady State Irradiance of $600\ W/m^2$:* Fig. 8 shows the output parameters of the PV array viz; PVpower, PVcurrent and PV voltage and the tracking performance of the P&O MPPT technique under the. steady state condition of irradiance of $600\ W/m^2$.

The behaviour of the boost converter at $600\ W/m^2$ is shown in Fig. 9. Where the DC link voltage is presented. It is inferred from waveforms that the converter operates in CCM, irrespective of variation in solar irradiance.

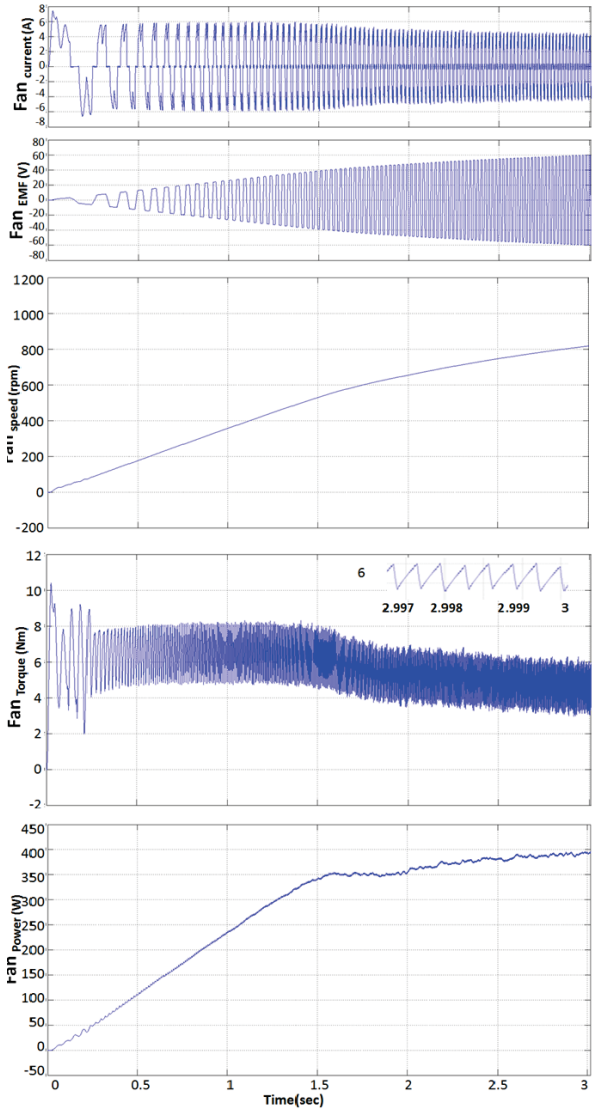


Fig. 6 BLDC-motor fan blower parameters at irradiance of 1000 $W/m^2$

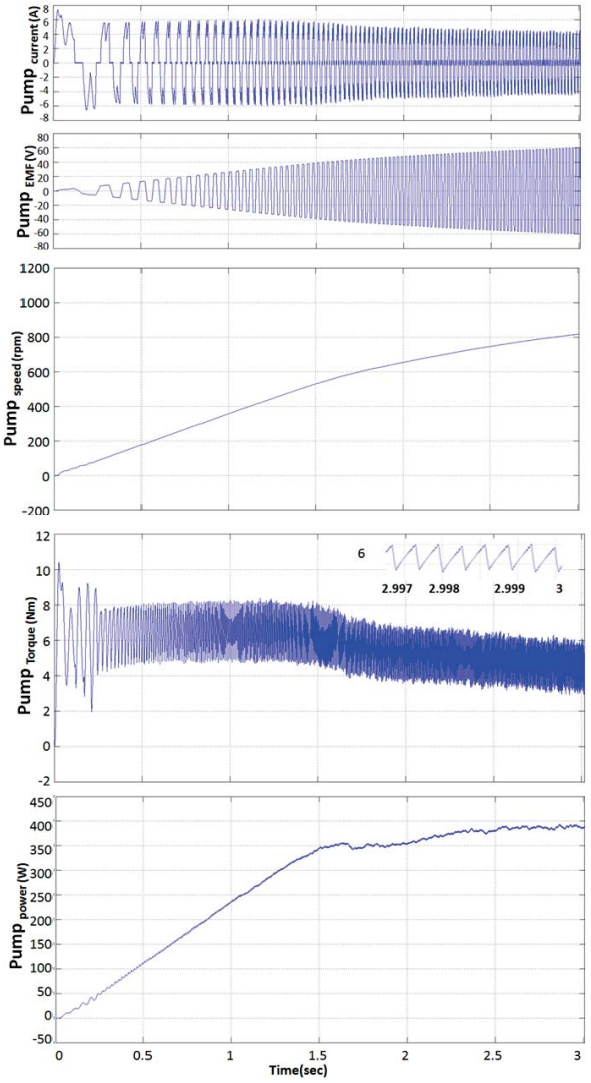


Fig. 7 BLDC-motor - water pump parameters at irradiance of 1000 $W/m^2$

*2) Performance of BLDC Motor at Steady State Irradiance of* 600 $W/m^2$*:* Performance of the BLDC motor with boost converter for motor - pump and fan blower is shown in Figs. 10 and 11 and the following points are clearly observed from the presented simulation results. The variables viz. the stator current, the back EMF, the rotor speed, the electromagnetic torque and the output power are plotted against time and the following inferences are noted:

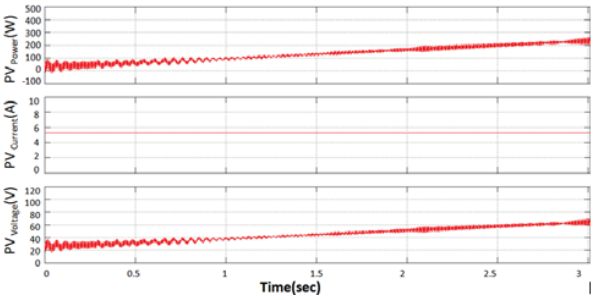


Fig. 8 Output parameters of the PV at irradiance of 600 $W/m^2$

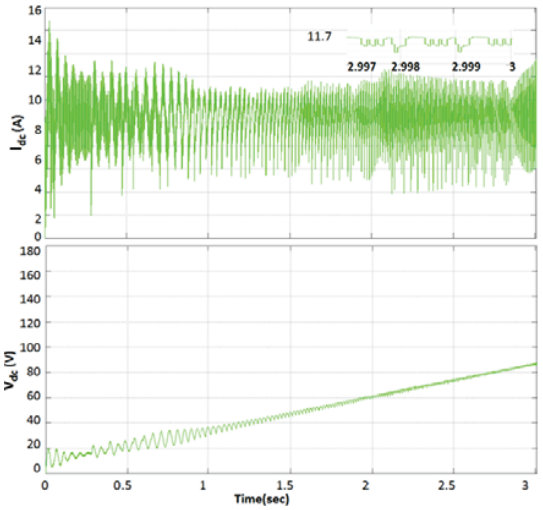


Fig. 9 Output parameters of boost converter at at irradiance of 600 $W/m^2$

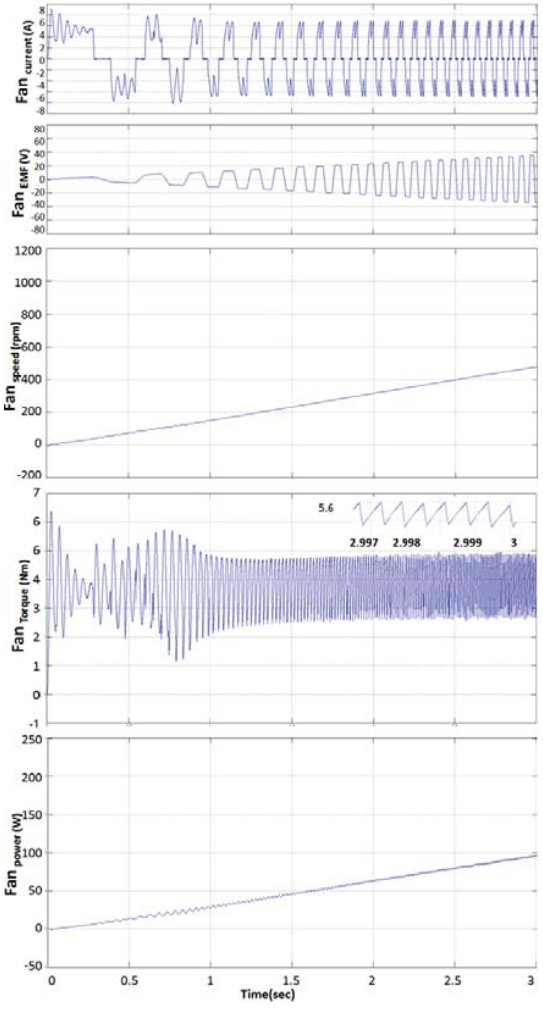


Fig. 10 BLDC-motor - fan blower parameters at irradiance of 600 $W/m^2$

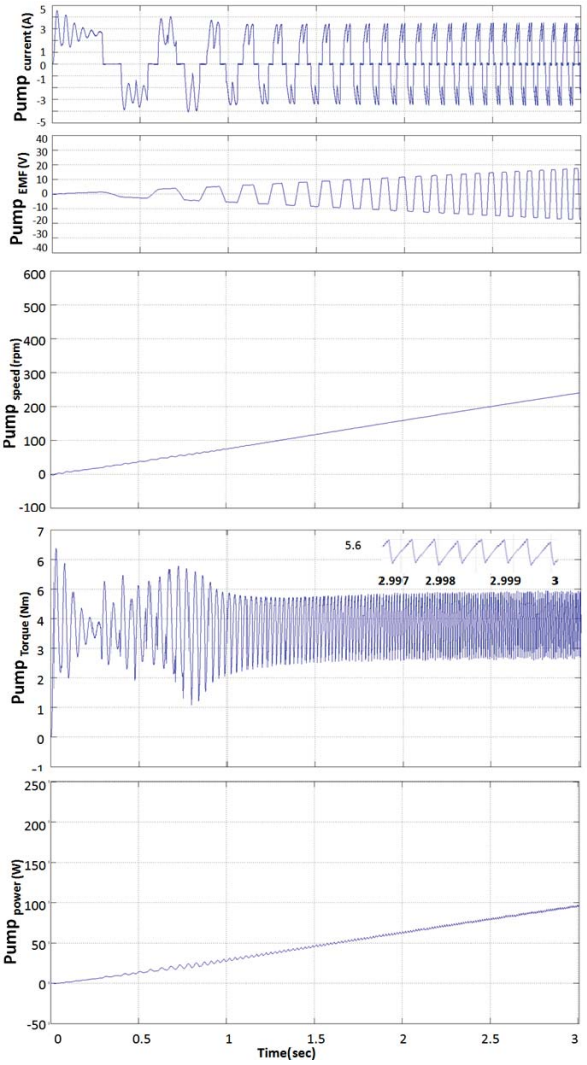


Fig. 11 BLDC-motor - water pump parameters at irradiance of 600 $W/m^2$

## VIII. Conclusion

The main aim of the proposed system is to attain comfort level during summer for the people living in the rural areas where it is difficult to depend on the electricity for all the time. The performance analysis has demonstrated with the novel features of proposed system such as proper design of SPV array, a new SMM based MPPT controller with boost converter, speed control of BLDC motor by variable DC link voltage and soft starting of the motor by wisely tracking the MPP and electronic commutation with fundamental frequency switching. The boost converter, having the advantage of very good conversion efficiency is found to be more suitable for the proposed air cooling system. The MATLAB/Simulink based simulation results displays superior outputs thus exhibiting the suitability of the proposed system, regardless of the environmental conditions.

## REFERENCES

[1] J. T. Bialasiewicz, "Renewable energy systems with photovoltaic power generators: pperation and modeling," *IEEE Transactions on Industrial Electronics,* Vo1. 55, No.7, 2752-2758 (2008).
[2] Li Tianze, Lu Hengwei, Jiang Chuan, Hou Luan, Zhang Xia , Application and design of solar photovoltaic system *International Photonics & Opto Electronics Meetings*, (2010).
[3] Jain, S., Thopukara, A. K. , Karampuri, R., and Somasekhar, V. T., A Single-stage photovoltaic system for a dual-inverter-fed open-end winding induction motor drive for pumping applications, *IEEE Transactions on Power Electronics*, Vol. 30, No. 9, 4809 - 4818 (2015).
[4] Le An and Lu, D. D. C., Design of a Single-Switch DC/DC Converter for a PV-Battery-Powered Pump System With PFM+PWM Control, *IEEE Transactions on Industrial Electronics*, Vol. 62, No. 2, 910 - 921, (2015).
[5] J. V. Mapurunga Caracas, G. De Carvalho Farias, L. F. Moreira Teixeira, and L. A. De Souza Ribeiro, Implementation of a high-efficiency, high-lifetime, and low-cost converter for an autonomous photovoltaic water pumping system, *IEEE Transactions on Industry Applications,* Vol. 50, No. 1, 631-641 (2014).
[6] Rajan Kumar and Bhim Singh, BLDC Motor Driven Water Pump Fed by Solar Photovoltaic Array Using Boost Converter, IEEE INDICOON.
[7] M. H. Taghvaee, M. A. M. Radzi, S. M. Moosavain, Hashim Hizam, and M. Hamiruce Marhaban, A current and future study on nonisolated DCDC converters for photovoltaic applications, *Renewable and Sustainable Energy Reviews*, Vol. 17, 216-227 (2013).
[8] Trishan Esram and Patrick L. Chapman, Comparison of photovoltaic array maximum power point tracking Techniques, *IEEE Transactions on Energy Conversion*, Vol. 22, No. 2, (2007).
[9] B. Subudhi and R. Pradhan, A Comparative Study on Maximum Power Point Tracking Techniques for Photovoltaic Power Systems, *IEEE Transactions on Sustainable Energy*, Vol. 4, No. 1, 89-98 (2013).
[10] B. Goldvin Sugirtha Dhas and S. N. Deepa, "Fuzzy logic based dynamic sliding mode control of boost inverter in photovoltaic application," *Journal of Renewable and Sustainable Energy,* Vol. 7, Issue 4, 043133 (2015); doi: 10.1063/1.4928737
[11] Mohamed M. Algazar, Hamdy AL-monier, Hamdy Abd EL-halim, and Mohamed Ezzat El Kotb Salem, Maximum power point tracking using fuzzy logic control, International Journal of Electrical Power & Energy Systems, vol. 39, Issue 1, 21-28(2012).
[12] R. Kumar and B. Singh, BLDC motor driven solar PV array fed water pumping system employing zeta converter, *IEEE India International Conference on Power Electronics,* 16 (2014).
[13] M. Uno and A. Kukita, Single-switch voltage equalizer using multistacked buckboost converters for partially-shaded photovoltaic modules, *IEEE Transactions on Power Electronics*, Vol. 30, No. 6, 30913105 (2015).
[14] S. A. K. H. Mozaffari Niapour, S. Danyali, M. B. B. Sharian, and M. R. Feyzi, Brushless dc motor drives supplied by PV power system based on Z-sourceinverterandFL-ICMPPTcontroller, *Energy Conversion and Management,* Vol. 52, No. 89, 30433059 (2011).
[15] M. Ouada, M.S. Meridjet, and N. Talbi, Optimization photovoltaic pumping system based BLDC using fuzzy logic MPPT control, *International Renewable and Sustainable Energy Conference*, 27-31 (2013).
[16] Aashoor, F. A. O. and Robinson, F. V. P., Maximum power point tracking of photovoltaic water pumping system using fuzzy logic controller, *International Universities' Power Engineering Conference*, 1-5 (2013).
[17] Emilio Mamarelis, Giovanni Petrone, and Giovanni Spagnuolo, Design of a sliding-mode-controlled SEPIC for PV MPPT applications, *IEEE Transactions on Industrial Electronics*, Vol. 61, No.7, 3387-3398 (2014).